American Mineralogist, Volume 80, pages 941–946, 1995

Anisotropic thermal expansion of calcite at high pressures: An in situ X-ray diffraction study in a hydrothermal diamond-anvil cell

TZY-CHUNG WU, ANDY H. SHEN,* MAURA S. WEATHERS, WILLIAM A. BASSETT
Mineral Physics Laboratory, Department of Geological Sciences, Snee Hall, Cornell University, Ithaca, New York 14853, U.S.A.

I-MING CHOU
U.S. Geological Survey, 959 National Center, Reston, Virginia 22092, U.S.A.

ABSTRACT

Lattice parameters of calcite were measured at simultaneous high pressures and temperatures up to 10 kbar and 500 °C. Samples of Solnhofen limestone and distilled, deionized water were loaded in a hydrothermal diamond-anvil cell. In situ energy-dispersive X-ray diffraction was used to determine lattice parameters along five H_2O isochores with densities of 1.040, 0.964, 0.760, 0.670, and 0.595 g/cm³ from 30 to 500 °C; these densities correspond to the ice-melting temperature of −7.7 °C and the liquid-vapor homogenization temperatures 92.4, 274.5, 318.9, and 344.6 °C, respectively. In addition, data along the P axis were collected by hydrostatic compression at room temperature and along the T axis by heating at atmospheric pressure. Our results show that anisotropic thermal expansion of calcite continues up to 10 kbar, therefore making it a good double internal X-ray standard. Both a and c lattice parameters are fitted to second-order polynomials of pressure, temperature, and a cross term.

INTRODUCTION

The thermal expansion of calcite has been extensively studied at 1 bar pressure (Chessin et al., 1965; Rao et al., 1968; Mirwald, 1979; Markgraf and Reeder, 1985). It was found that the **a** axis shows a small negative thermal expansion and the **c** axis shows a large positive expansion. A tricritical orientational order-disorder transition at 987 °C is thought to be the cause of the anomalous thermal behavior of calcite at lower temperature (Dove and Powell, 1989). Under compression at room temperature, both the a and c lattice parameters of calcite show a normal decrease (Merrill and Bassett, 1975; Fiquet et al., 1994). This anisotropic thermal expansion of calcite has not only been a challenge for understanding the lattice dynamics responsible for it (Dove et al., 1992) but has also been proposed as a possible double internal X-ray standard for pressure and temperature in a single phase (Hazen and Finger, 1982).

Although many studies have investigated thermal expansion and compressibility, there are virtually no data at simultaneous high pressures (P) and temperatures (T). The reason is partly because of a lack of means to measure pressure and temperature simultaneously with satisfactory precision and accuracy for in situ lattice parameter measurement. This capability has been recently made possible by the development of a hydrothermal diamond-anvil cell (HDAC) (Bassett et al., 1993). With X-rays from a synchrotron source, the HDAC can be used to perform in situ X-ray diffraction to study mineral properties and reactions (e.g., Huang et al., 1994). In this paper we present the results of lattice parameter determinations of calcite at simultaneous high pressures and temperatures using an HDAC.

EXPERIMENTAL METHODS AND PROCEDURES

The HDAC used in high-P and -T experiments was equipped with two resistance heaters surrounding the upper and lower diamonds, and two K-type (Ni chromel–Ni alumel) thermocouples attached to the pavilion faces for measuring the temperatures of both diamonds. The thermocouples were calibrated against the ice I–ice III–liquid triple point (−21.985 °C), the ice I–liquid–vapor triple point (0.01 °C), and the melting points of sodium nitrate (306.8 °C) and sodium chloride (800.5 °C) at 1 bar. Because the thermocouples were not under any compression, no correction for pressure-induced error was needed. In this design, the voltage of either heater can be adjusted by a variable resistor. The temperature difference between the two diamonds can be controlled to within 1 °C throughout the experiments.

Solnhofen limestone was used as the source of calcite because of its fine grain size (1–10 μm). In these experiments, the polycrystalline aggregate was preferred over powder because it remains intact, allowing visual observation of the air bubble for measurement of the homogenization temperatures of the H_2O fluid. The sample and

* Present address: Bayerisches Geoinstitut, Universität Bayreuth, D-95440 Bayreuth, Germany.

0003–004X/95/0910–0941$02.00

TABLE 1. Densities of H_2O fluid-pressure medium in isochoric experiments

Sample no.	Measured T (°C)	Density (g/cm³)
	T_h*	
411-1	92.4	0.964
410-3	274.5	0.760
410-2	318.9	0.670
410-1	344.6	0.595
	T_m**	
411-3	−7.7	1.040

* T_h is the liquid-vapor homogenization temperature of H_2O.
** T_m is the melting temperature of solid H_2O, ice I.

TABLE 2. Normalized unit-cell parameters of calcite at high pressures and temperatures

T (°C)	P (bar)	a/a_0	c/c_0	V/V_0
		Density = 1.040 g/cm³		
404(2)	8671(39)	0.9944(10)	1.0015(14)	0.990(2)
304(2)	6636(44)	0.9953(12)	1.0009(16)	0.992(3)
203(2)	4419(45)	0.9966(9)	1.0000(13)	0.993(2)
102(2)	2249(39)	0.9982(9)	0.9989(11)	0.995(2)
30(1)	1121(6)	0.9990(12)	0.9978(10)	0.996(3)
		Density = 0.964 g/cm³		
503(2)	7585(33)	0.9933(16)	1.0053(21)	0.992(4)
404(2)	5842(35)	0.9962(13)	1.0066(15)	0.999(3)
304(2)	3969(36)	0.9970(12)	1.0060(13)	1.000(3)
203(2)	1985(36)	0.9983(12)	1.0049(10)	1.001(3)
102(2)	142(29)	0.9997(15)	1.0031(14)	1.003(3)
30(1)	1	1	1	1
		Density = 0.760 g/cm³		
506(2)	2883(21)	0.9975(16)	1.0062(11)	1.001(4)
405(2)	1658(22)	0.9977(18)	1.0055(13)	1.001(4)
304(2)	413(22)	0.9983(16)	1.0044(11)	1.001(3)
200(2)	1	0.9990(18)	1.0029(23)	1.001(3)
100(2)	1	0.9997(17)	1.0009(14)	1.000(4)
30(0.2)	1	1	1	1
		Density = 0.670 g/cm³		
506(2)	1863(16)	0.9979(15)	1.0134(13)	1.009(3)
405(2)	905(16)	0.9984(15)	1.0106(13)	1.007(3)
304(2)	1	0.9989(13)	1.0084(12)	1.006(3)
200(2)	1	0.9993(15)	1.0055(13)	1.004(3)
100(2)	1	0.9996(12)	1.0015(13)	1.001(3)
30(0.2)	1	1	1	1
		Density = 0.595 g/cm³		
506(2)	1336(13)	0.9980(8)	1.0116(6)	1.008(2)
405(2)	581(13)	0.9981(8)	1.0104(6)	1.007(2)
304(2)	1	0.9992(13)	1.0061(14)	1.005(3)
200(2)	1	0.9995(19)	1.0044(24)	1.003(4)
100(2)	1	0.9999(7)	1.0020(6)	1.002(2)
30(0.2)	1	1	1	1
		Room temperature compression		
30(0.2)	1800(1000)	0.9986(12)	0.9990(11)	0.996(3)
30(0.2)	6700(1000)	0.9966(12)	0.9942(10)	0.988(3)
30(0.2)	8800(1000)	0.9959(12)	0.9935(10)	0.985(2)
		Ambient pressure heating		
30(2)	1	1	1	1
100(2)	1	0.9995(15)	1.0025(26)	1.001(3)
200(2)	1	0.9991(14)	1.0055(26)	1.004(3)
400(2)	1	0.9985(15)	1.0115(26)	1.009(3)
432(2)	1	0.9983(15)	1.0131(27)	1.010(3)
524(2)	1	0.9982(15)	1.0164(27)	1.013(3)

Note: numbers in parentheses are uncertainties for temperatures and pressures and are standard deviation for normalized unit-cell parameters. The unit-cell parameters for the starting sample are a_0 = 4.983 ± 0.011, c_0 = 17.035 ± 0.039 Å.

distilled, deionized H_2O were loaded into the sample chamber, which was made by drilling a 500 μm hole in a 125 μm thick Re foil. The sample chamber was then quickly sealed by lowering the upper plate of the diamond cell. During the normal loading procedure, an air bubble is trapped in the chamber. The ratio of the volume of air bubble to that of liquid H_2O determines the density of the fluid after homogenization. If no bubble is trapped, then the density of the fluid is >1 g/cm³.

In the HDAC, the pressure evolution during a heating experiment is constrained by the equation of state of H_2O. As the temperature is increased, the pressure follows the liquid-gas coexistence boundary of the fluid before the bubble and the liquid homogenize. As the temperature of the sample and homogenized fluid is increased, the pressure in the sample chamber increases following one isochore of the fluid, provided that the volume (V) of the fluid stays constant. The volume of the sample chamber was monitored by laser interferometry (Shen et al., 1993) when homogenization temperature was measured. These observations confirmed that the volume of the sample chamber remained constant to within 1.5% during heating and to within 0.5% during cooling in the HDAC when the gaskets used were pretreated at high temperature. The isochoric density of the fluid must be determined to calculate the pressure from the measured temperature. If the density of the fluid is <1 g/cm³ (i.e., a bubble exists after sealing the cell), then the homogenization temperature can be used to determine the density on the basis of the volumetric relationship of H_2O (Wagner and Pruss, 1993). If the density of the fluid is >1 g/cm³, i.e., no bubble exists, the density can be determined from the PVT relations along the liquidus of H_2O (Wagner et al., 1994). Once the fluid density is known, and if the volume of the sample chamber is constant, the pressure can be calculated from the temperature by using the equation of state of H_2O (Haar et al., 1984).

Real-time energy-dispersive X-ray diffraction was used to analyze samples at high pressure and temperature at the B-1 station of the Cornell High Energy Synchrotron Source (CHESS). An intrinsic Ge solid-state detector and a multichannel analyzer were used to record the diffraction signal as an energy spectrum, which was calibrated with ^{55}Fe and ^{133}Ba radiation sources. The 2θ diffraction angle for all experiments was approximately 12° and was calibrated with Au foil. The average accumulation time for a diffraction pattern was 2 min.

For isochoric experiments, we typically heated the cell up to 500 °C from room temperature within 5 min. X-ray diffraction patterns were collected at 100 °C intervals during cooling. The temperature was controlled to within ±2 °C of the desired temperature during the collection of diffraction patterns. After each heating and cooling cycle, a diffraction pattern was collected at 1 bar and room temperature as the normalization standard for each isochore.

For the compression experiment at room temperature,

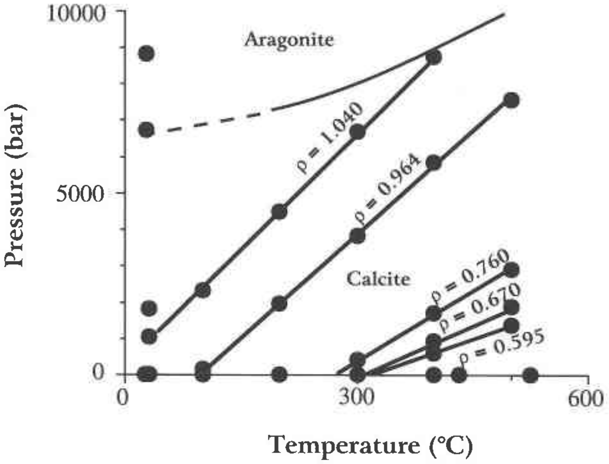

Fig. 1. The pressure-temperature conditions at which the X-ray diffraction patterns were collected (solid circles), together with the stability fields of calcite and aragonite. The lines connecting data points are isochores of H_2O fluid, with densities labeled next to them in grams per cubic centimeter.

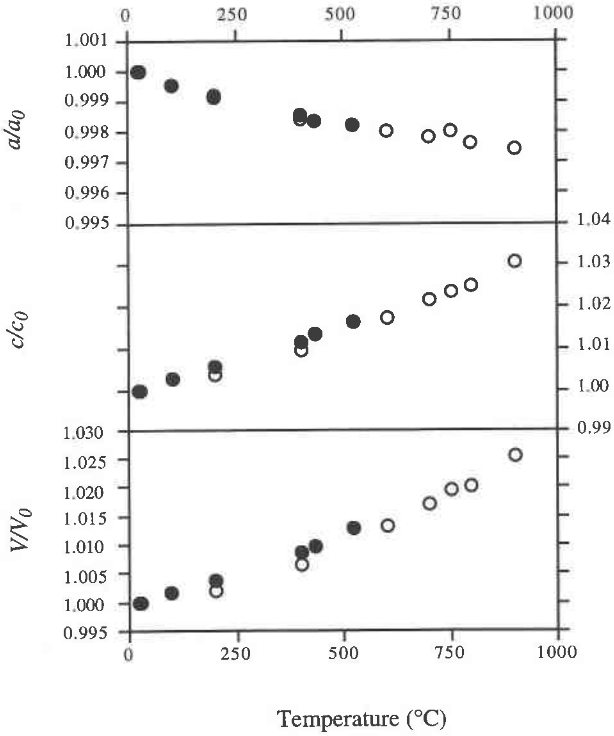

Fig. 2. Anisotropic thermal expansion data at 1 bar pressure from this study (solid circles) are plotted with the data of Markgraf and Reeder (1985) (open circles).

we used a methanol-ethanol-water mixture as the pressure medium. The shift of the R1 line of ruby fluorescence was used to determine pressure (Mao et al., 1986). The optical spectra of ruby fluorescence excited by 488 nm light from an Ar ion laser were collected before and after each collection of diffraction patterns.

The high-*T*, ambient-*P* experiment was done on a Scintag X-ray diffractometer with θ-θ geometry. Samples were heated in a Buehler high-temperature chamber mounted on the diffractometer, and the temperature was measured using an S-type (Pt-Pt10%Rh) thermocouple.

Results and discussion

High-*P* and -*T* isochoric experiments were conducted along five isochores of H_2O fluid. The observed homogenization temperature (T_h), or ice-melting temperature (T_m), and the corresponding densities of isochores are listed in Table 1. The temperatures and pressures at which the X-ray diffraction patterns were collected are listed in Table 2 and plotted in Figure 1. The stability fields of calcite and aragonite are also shown in Figure 1. The uncertainties associated with those points are listed in parentheses in Table 2. Uncertainties of temperature indicate the range of temperature variation during data collection. Uncertainties of pressure reflect the temperature variation and the uncertainties from the equation of state of H_2O.

All the diffraction peaks were fitted with Gaussian peak functions to obtain the peak position. The positions of $01\bar{1}2$, $10\bar{1}4$, $11\bar{2}0$, $11\bar{2}3$, $20\bar{2}2$, $01\bar{1}8$, and $11\bar{2}6$ peaks of calcite were used to obtain unit-cell parameters by least-squares fitting. The fitted lattice parameters and unit-cell volume were normalized to the value at ambient pressure and temperature. The standard deviations were calculated for data points during the least-square fitting and were propagated to the normalized values.

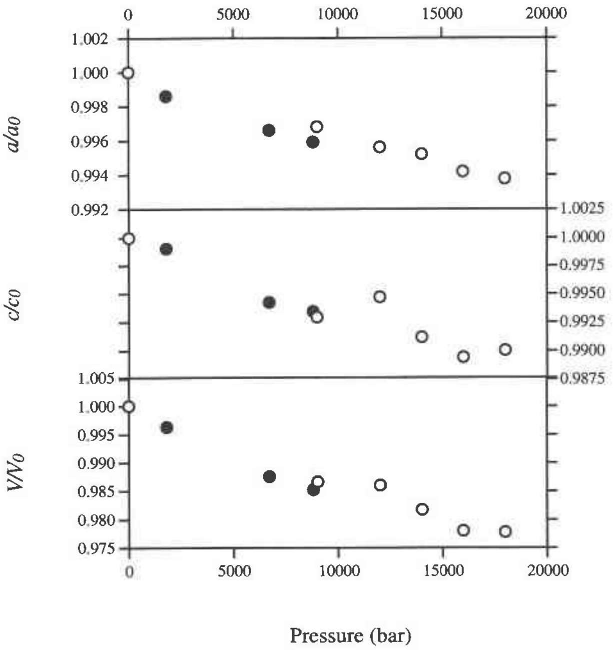

Fig. 3. Room temperature compression data from this study (solid circles) are plotted with the data of Fiquet et al. (1994) (open circles).

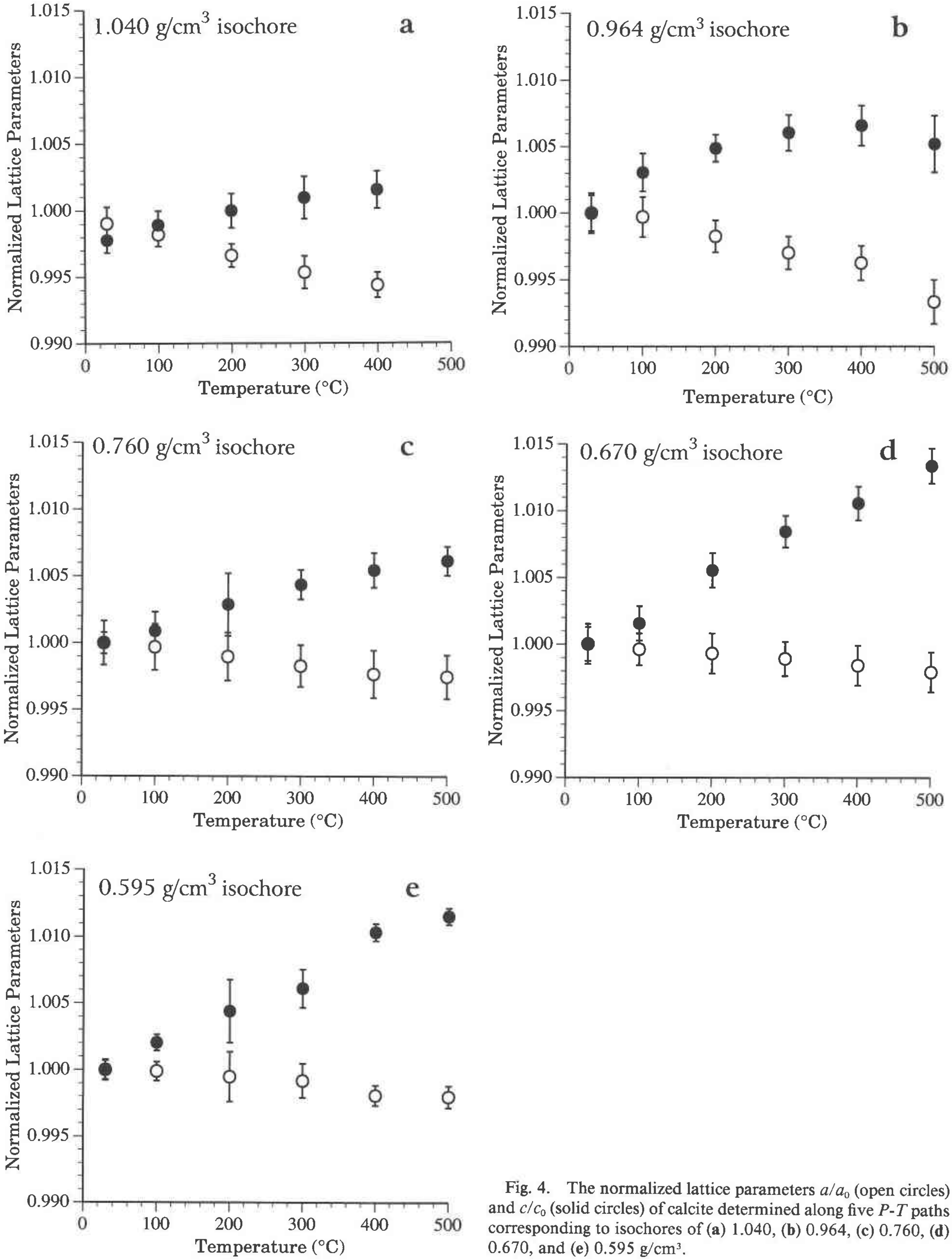

Fig. 4. The normalized lattice parameters a/a_0 (open circles) and c/c_0 (solid circles) of calcite determined along five P-T paths corresponding to isochores of (**a**) 1.040, (**b**) 0.964, (**c**) 0.760, (**d**) 0.670, and (**e**) 0.595 g/cm³.

The thermal expansion data at 1 bar pressure determined in this study are plotted and compared with those of Markgraf and Reeder (1985) in Figure 2. Room temperature compression data are plotted and compared with those of Fiquet et al. (1994) in Figure 3. Both show good agreement with those previous studies. The normalized lattice parameters a/a_0 and c/c_0 at simultaneous high pressures and temperatures along each H_2O isochore are plotted in Figure 4.

Lattice parameters of calcite as a function of pressure and temperature

The variation of both a and c can be fitted to a linear combination of second-order polynomials of pressure and temperature without any cross terms. That is, both thermal expansion and compression of these two unit-cell parameters can be represented by second-order polynomials, and the simultaneous effect of P and T can be described by the sum of the two. A cross $P \cdot T$ term can be added to the fitting model, which combines the pressure dependence of the first-order temperature derivative and the temperature dependence of the first-order pressure derivative. With the $P \cdot T$ term added, the goodness of fitting, indicated by the degree of freedom (DOF) adjusted r^2, improves slightly for both c/c_0 and a/a_0. Adding higher-order cross terms, $P \cdot T^2$, $P^2 \cdot T$, or $P^2 \cdot T^2$, to the equations did not lead to any further improvement. The fitted parameters of the polynomial equations with the $P \cdot T$ cross term added are listed in Table 3. Figure 5 shows the data of a/a_0 and c/c_0 along the vertical axis with temperature and pressure on the horizontal axes. The surfaces of the fitted polynomials are also plotted in Figure 5. Because the best fits for both lattice parameters resulted from the application of the second-order polynomial equations with a small coefficient for the $P \cdot T$ cross term, we conclude that thermal expansion has a pressure dependence, and that compression has a temperature dependence, although both are small.

Anisotropic thermal expansion at high pressures

On the basis of the structure refinement data, Markgraf and Reeder (1985) explained the negative thermal expansion of the **a** axis as a result of the unusually large libration motion of CO_3 groups about the threefold axis. The basal octahedral edge, the O1-O2 of CaO_6 [see Reeder (1983) for the number index of O atoms in the octahedron], shows contraction corresponding to increasing libration motion of CO_3 groups as the temperature rises. We undertook our measurements in part to determine if the increasing interaction between CO_3 groups under high pressures might change the thermal expansion behavior. However, our results clearly show that both axes retain thermal expansion behavior at high pressures similar to behavior at 1 bar pressure. Apparently, increasing pressure up to ~10 kbar does not significantly change the thermoelastic behavior of calcite.

Dove and Powell (1989) have shown that at 1 bar pressure the anomalously large thermal expansion of the **c**

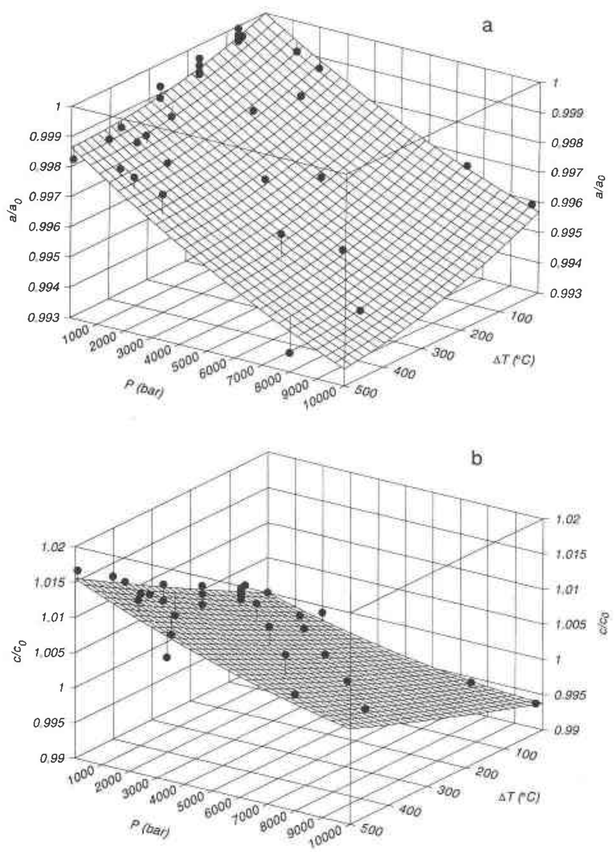

Fig. 5. Three-dimensional plots showing the measured normalized lattice parameters a/a_0 and c/c_0 of calcite (**a** and **b**, respectively) as a function of pressure and temperature. The polynomial equations obtained from the least-squares fitting to the data are also plotted as three-dimensional surfaces.

TABLE 3. Least-squares fitting results of the unit-cell parameters as a function of pressure and temperature

Normalized unit-cell parameters	$a \times 10^6$	$b \times 10^9$	$c \times 10^7$	$d \times 10^{11}$	$e \times 10^{10}$	DOF adj. r^2
a/a_0	−5.398	5.371	−5.741	1.412	−1.528	0.963
c/c_0	28.798	4.367	−11.110	4.662	−11.151	0.942
V/V_0	13.319	18.280	−22.155	5.414	−7.339	0.945

Note: the data are fitted to the polynomial $x/x_0 = 1 + a\Delta T + b(\Delta T)^2 + cP + dP^2 + eP\Delta T$, where x is one of the unit-cell parameters and $\Delta T = T$ (°C) − 30. The least-squares fittings are weighted according to the standard deviation of each normalized unit-cell parameter.

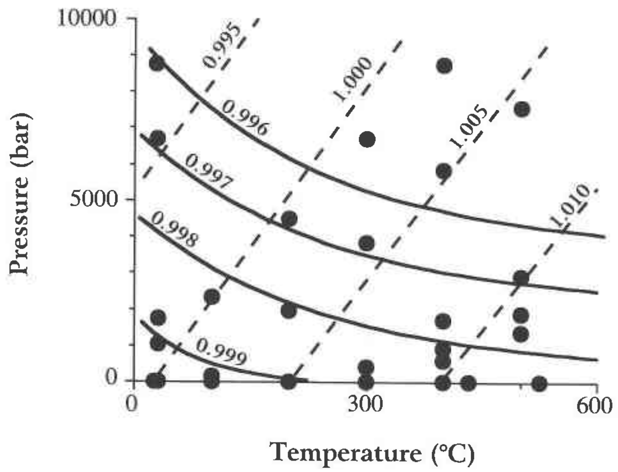

Fig. 6. Contour lines of normalized lattice parameters a/a_0 (solid lines) and c/c_0 (dashed lines) of calcite plotted in P-T space, together with data points (solid circles).

axis can be explained by a spontaneous strain associated with the high-temperature order-disorder transition. On the basis of our data, we suggest that the dependence of the spontaneous strain on pressure is small within the range of our measurement. A precise measurement of the transition boundary at higher pressure and more data at higher temperature near the transition boundary are necessary to conduct meaningful analysis of the exact pressure dependence of the spontaneous strain and the order parameters.

PVT relationship of calcite

At room temperature, Fiquet et al. (1994) used the Birch-Murnaghan equation of state to describe the compression behavior of calcite. Because calcite exhibits an anisotropic behavior that differs significantly from the isotropic behavior of most materials to which the Birch-Murnaghan equation of state for solids is best applied, we choose to use an empirical polynomial equation to describe the compression behavior at high temperature. The fitted parameters of V/V_0 are also listed in Table 3.

Calcite as a double internal X-ray standard

Because we have demonstrated that calcite maintains anisotropic thermal expansion at high pressure, calcite can indeed be used as a double internal X-ray standard. For any combination of measured a and c axial lengths, there can be only one possible pressure and temperature. The approximate contour lines for a/a_0 and c/c_0 are plotted in a P-T diagram in Figure 6. This plot can be compared to that predicted by Hazen and Finger (1982), with the typographic errors in their diagram corrected. Our data show that the contour lines of c/c_0 have a trend similar to theirs, and the contour lines of a/a_0 have a larger curvature than they predicted. The application of the polynomial formula (Table 3), however, should be limited to the P-T range of our data, 0–10 kbar and 25–500 °C, respectively.

Acknowledgments

We thank Howard T. Evans, Jr., Gordon L. Nord, Jr., and G. Fiquet for their constructive comments. We also wish to thank the staff at the Cornell High Energy Synchrotron Source (CHESS) for their help in our experiments. This work was supported by National Science Foundation grant EAR-9304894.

References cited

Bassett, W.A., Shen, A.H., Bucknum, M.J., and Chou, I-M. (1993) A new diamond anvil cell for hydrothermal studies to 2.5 GPa and from −190 to 1200 °C. Review of Scientific Instruments, 64, 2340–2345.

Chessin, N., Hamilton, W.C., and Post, B. (1965) Position and thermal parameters of oxygen atoms in calcite. Acta Crystallographica, 18, 689–693.

Dove, M.T., and Powell, B.M. (1989) Neutron diffraction study of the tricritical orientational order/disorder phase transition in calcite at 1260 K. Physics and Chemistry of Minerals, 16, 503–507.

Dove, M.T., Hagen, M.E., Harris, M. J., Powell, B.M., Steigenberger, U., and Winkler, B. (1992) Anomalous inelastic neutron scattering from calcite. Journal of Physics: Condensed Matter, 4, 2761–2774.

Fiquet, G., Guyot, F., and Itié, J.-P. (1994) High-pressure X-ray diffraction study of carbonates: $MgCO_3$, $CaMg(CO_3)_2$, and $CaCO_3$. American Mineralogist, 79, 15–23.

Haar, L., Gallagher, J.S., and Kell, G.S. (1984) NBS/NRC steam tables: Thermodynamic and transport properties and computer programs for vapor and liquid states of water in SI units, 320 p., Hemisphere, Washington, DC.

Hazen, R.M., and Finger, L.W. (1982) Comparative crystal chemistry, 231 p., Wiley, New York.

Huang, W.-L., Bassett, W.A., and Wu, T.-C. (1994) Dehydration and hydration of montmorillonite at elevated temperatures and pressures monitored using synchrotron radiation. American Mineralogist, 79, 683–691.

Mao, H.K., Xu, J., and Bell, P.M. (1986) Calibration of the ruby pressure gauge to 800 kbar under quasi-hydrostatic conditions. Journal of Geophysical Research, 91, 4673–4676.

Markgraf, S.A., and Reeder, R.J. (1985) High temperature structure refinements of calcite and magnesite. American Mineralogist, 70, 590–600.

Merrill, L., and Bassett, W.A. (1975) The crystal structure of $CaCO_3$(II), a high-pressure metastable phase of calcium carbonate. Acta Crystallographica, B31, 343–349.

Mirwald, P.W. (1979) Determination of a high-temperature transition of calcite at 800 degrees C and one bar carbon dioxide pressure. Neues Jahrbuch für Mineralogie Monatshefte, 7, 309–315.

Rao, K.V.K., Naidu, S.V.N., and Murthy, K.S. (1968) Precision lattice parameters and thermal expansion of calcite. Journal of Physics and Chemistry of Solids, 29, 245–248.

Reeder, R.J. (1983) Crystal chemistry of rhombohedral carbonates. In R.J. Reeder, Ed., Carbonates: Mineralogy and chemistry, p. 1–47. Mineralogical Society of America, Washington, DC.

Shen, A.H., Bassett, W.A., and Chou, I-M. (1993) The α-β quartz transition at high temperatures and pressures in a diamond-anvil cell by laser interferometry. American Mineralogist, 78, 694–698.

Wagner, W., and Pruss, A. (1993) International equations for the saturation properties of ordinary water substance. Revised according to the international temperature scale of 1990. Addendum to Journal of Physical and Chemical Reference Data 16, 893 (1987). Journal of Physical and Chemical Reference Data, 22, 783–787.

Wagner, W., Saul, A., and Pruss, A. (1994) International equation for the pressure along the melting and the sublimation of ordinary water substance. Journal of Physical and Chemical Reference Data, 23, 515–527.

Manuscript received January 20, 1995
Manuscript accepted May 23, 1995